

The Delicate Electronic and Magnetic Structure of the LaOFePn System (Pn = pnictogen)

S. Lebègue*,¹ Z. P. Yin*,² and W. E. Pickett²

¹ *Laboratoire de Cristallographie et de Modélisation des Matériaux Minéraux et Biologiques,*

UMR 7036, CNRS-Université Henri Poincaré,

B.P. 239, F-54506 Vandoeuvre-lès-Nancy, France

² *Department of Physics, University of California Davis, Davis, CA 95616*

(Dated: February 10, 2022)

* These authors contributed equally to this work.

Abstract

The occurrence of high temperature superconductivity, and the competition with magnetism, in stoichiometric and doped LaOFeAs and isostructural iron-oxypnictides is raising many fundamental questions about the electronic structure and magnetic interactions in this class of materials. There are now sufficient experimental data that it may be possible to identify the important issues whose resolution will lead to the understanding of this system. In this paper we address a number of the important issues. One important characteristic is the Fe-As distance (or more abstractly the pnictogen (Pn) height $z(\text{Pn})$); we present results for the effect of $z(\text{Pn})$ on the electronic structure, energetics, and Fe magnetic moment. We also study LaOFeAs under pressure, and investigate the effects of both electron and hole doping within the virtual crystal approximation. The electric field gradients for all atoms in the LaOFeAs compound are presented (undoped and doped) and compared with available data. The observed (π, π, π) magnetic order is studied and compared with the computationally simpler $(\pi, \pi, 0)$ order which is probably a very good model in most respects. We investigate the crucial role of the pnictogen atom in this class, and predict the structures and properties of the N and Sb counterparts that have not yet been reported experimentally. At a certain volume a gap opens at the Fermi level in LaOFeN, separating bonding from antibonding bands and suggesting directions for a better simple understanding of the seemingly intricate electronic structure of this system. Finally, we address briefly on the possible effects of post-lanthanum rare earths, which have been observed to enhance the superconducting critical temperature substantially.

PACS numbers:

I. BACKGROUND AND MOTIVATION

Isostructural and isovalent LaOFeP and LaOFeAs are layered conductors, the first being superconducting at $T_c=2.5$ K¹ while the second becomes antiferromagnetically ordered at $T_N \approx 140$ K^{2,3} and is not superconducting. The discovery of superconductivity at 26 K in carrier-doped LaOFeAs⁴, followed by rapid improvement now up to $T_c=55$ K⁵ in this class, makes these superconductors second only to the cuprates in critical temperature. Several dozen preprints appeared within the two months after the original publication, and many hundred since, making this the most active field of new materials study in recent years (since the discovery in MgB₂, at least).

A host of models and ideas about the “new physics” that must be operating in this class of compounds is appearing, pointing out the need to establish a clear underpinning of the basic electronic (and magnetic) structure of the system. The materials are strongly layered, quasi-two-dimensional in their electronic structure, by consensus. The electronic structure of LaOFeP was described by Lebègue,⁶ with the electronic structure and its neighboring magnetic instabilities of LaOFeAs being provided by Singh and Du⁷. Several illuminating papers have appeared since, outlining various aspects of the electronic and magnetic structure of LaOFeAs.

The extant electronic structure work has provided a great deal of necessary information, but still leaves many questions unanswered, and indeed some important questions are unaddressed so far. In this paper we address some of these questions more specifically. Stoichiometric LaOFeAs is AFM; then ~ 0.05 carriers/Fe doping of either sign destroys magnetic order and impressive superconductivity arises, with T_c seemingly depending little on the carrier concentration. Another question is: with the nonmagnetic electronic structure of LaOFeP and LaOFeAs being so similar, why is the former superconducting while the latter is (antiferro)magnetic? Surely this difference must be understood and built into bare-bones models, or else such models risk explaining nothing, or explaining anything. Another question is the effect of the structure. Unusual sensitivity to the As height $z(\text{As})$ has been noted⁸; T_c is reported to increase with applied pressure^{9,10} (reduction in volume) for low values of doping (up to $x = 0.11$ in $\text{LaO}_{1-x}\text{F}_x\text{FeAs}$, which is reported as the amount of F for optimal

doping); there are increases in T_c due to replacement of La with other rare earth ions, and the variation in size of the rare earth is often a dominant factor in the observed trends in their compounds. Very important also is the magnetism in these materials, as magnetism is a central feature in the cuprate superconductors and in correlated electron superconductors. Another important question is: what can be expected if other pnictide atoms can be incorporated into this system: Sb (or even Bi) on the large atom side, or N on the small atom end. In this paper we address these questions.

II. CRYSTAL STRUCTURE

The members of the family of the new Fe-based superconductors crystallize in the ZrCuSiAs type structure^{11,12} (space group $P4/nmm$, $Z = 2$). For instance, LaOFeAs is made of alternating LaO and FeAs layers, as presented in Fig. 1. The Fe and O atoms lie in planes,

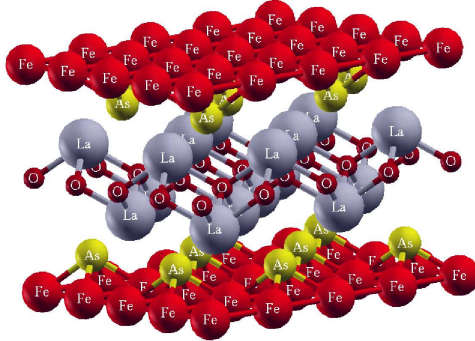


FIG. 1: (Color online) The crystal structure of LaOFeAs, showing the alternating layers of LaO and FeAs.

while the As and La atoms are distributed on each side of these planes following a chess-board pattern. The crystal structure is fully described by the a and c lattice parameters, together with the internal coordinates of La and As. Experimentally, $a = 4.03533 \text{ \AA}$ and $c = 8.74090 \text{ \AA}$, while $z(\text{La}) = 0.14154$ and $z(\text{As}) = 0.6512$. However to describe correctly the antiferromagnetic structure, a $\sqrt{2}a \times \sqrt{2}a \times c$ cell must be used, with four Fe atoms per cell, as shown in full lines in Fig. 2. We will refer to this antiferromagnetic order as

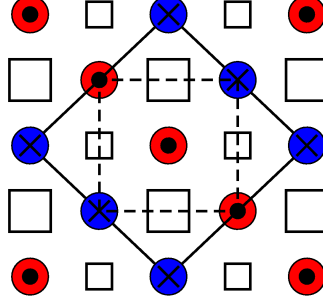


FIG. 2: (Color online) The Q_M magnetic structure of the Fe-As substructure of LaOFeAs, showing alternating chains of Fe spin up (red circles with black dots) and Fe spin down (blue circles with black crosses). The As atoms above (below) the Fe plane are represented as large (small) squares. The $\sqrt{2}a \times \sqrt{2}a \times c$ cell is represented in full lines, while the $a \times a \times c$ cell is in dashed lines.

the Q_M AFM order, or equivalently as $(\pi, \pi, 0)$, while the Q_0 AFM order corresponds to an antiferromagnetic order of the original cell (dashed lines in Fig. 2) with two Fe atoms. Also, FM will refer to a ferromagnetic arrangement of the spins, while NM means non-magnetic.

III. CALCULATION METHOD

To calculate the relevant quantities, we have used density functional theory (DFT)^{13,14}, as implemented in three different electronic structure codes. The full potential local orbital (FPLO) code^{15,16} was mainly used, while we double checked some of the calculations with Wien2k code¹⁷. For most of the FPLO and LAPW calculations, the Perdew and Wang 1992 (PW92)¹⁸ exchange-correlation (XC) functional was used, but the effect of XC functional was checked using also LSDA(PZ)¹⁹, the PBE (Perdew *et al.* 1996)²⁰, and another GGA (Perdew *et al.* 1992)²¹ XC functionals. At each constant volume, the crystal structure was fully relaxed, i.e., c/a , $z(\text{La})$ and $z(\text{Pn})$ were relaxed, where Pn is the pnictogen atom. The errors were estimated to be within 0.5% for c/a , and 1.0% for $z(\text{La})$ and $z(\text{Pn})$. The relaxation was performed in the Q_M AFM structure, with 132 irreducible k points in the BZ. We double checked the total energy with a finer mesh with 320 irreducible k points in the BZ, and the difference is very small. After relaxation, all calculations were performed

using dense meshes, with 320, 1027, and 637 irreducible k points in the BZ of the Q_M AFM, Q_0 AFM and NM structure, respectively. In the Q_M AFM structure, we used 464 irreducible k points in the BZ to double check the result, without any noticeable difference in the DOS nor band structure. As for the results presented in Sect. V, we used the PAW (projector augmented waves) method²² as implemented in the code VASP (Vienna Ab-initio Simulation Package)^{23,24}. The Perdew Burke Ernzerhof²⁰ variant of the generalized gradient approximation (GGA) was used for the exchange-correlation potential. A cut-off of 600 eV was used for the plane-wave expansion of the wave function to converge the relevant quantities. For Brillouin zone integrations, a mesh of $9 \times 9 \times 7$ k -points²⁵ was used within the modified tetrahedron method²⁶. This mesh was decreased to $9 \times 9 \times 3$ for the cell doubled along the c axis.

IV. STUDY OF LAOFEAS IN THE TETRAGONAL STRUCTURE

LaOFeAs has a tetragonal structure (as described in Sect. II) at room temperature⁴. Although it undergoes a structural phase transition at lower temperature^{2,3} (see Section V), the doped (and superconducting) material $\text{LaO}_{1-x}\text{F}_x\text{FeAs}$ remains in this structure down to low temperature, so the study of LaOFeAs in the high symmetry structure is a necessary step towards the understanding of the electronic structure of the whole family of compounds.

A. Influence of XC functionals and codes on the electronic structure of LaOFeAs

First, we studied the electronic structure of LaOFeAs in the experimental (tetragonal) crystal structure for different magnetic states (Q_M AFM, Q_0 AFM, FM and NM) using two different codes (FPLO7 and Wien2K) and different exchange-correlation functionals. This is necessary in view of the large number of theoretical papers^{7,27,28,29,30} which appeared recently and often contain strong disagreements. This was partly studied by Mazin *et al.*³¹ Table I summarizes the results: the magnetic moment on the Fe atom together with the total energy differences for each magnetic state studied here. Independent of the code or the XC functional used, the Q_M AFM state is always found to be the ground state, which

confirms our earlier report⁸. The magnetic moment for both AFM orders are considerably larger than the ordered moment reported from neutron diffraction and muon spin relaxation experiments, while the one for the FM order is much smaller. For this last case, FPLO7 gives zero which indicates no magnetism with both PZ and PW92 XC functional; Wien2K gives about $0.36 \mu_B$ with GGA and PBE and $0.13 \mu_B$ with PW92. It appears therefore that the magnetic moment of Fe for the same state with different XC functionals varies by up to $0.5 \mu_B$, which is unexpectedly large, although GGA is known to enhance magnetism.³¹ The difference between FPLO7 and Wien2K in predicting the Fe magnetic moment for each state may explain the total energy differences among them. Virtual doping (see subsection B) by $0.1 e^-/\text{Fe}$ enhances the Fe magnetic moment in the Q_M AFM state but reduces it in the FM state for all the XC functionals used.

In the structural optimization (performed in the Q_M state), FPLO7 with PW92 (LDA) functional gives reasonable c/a and $z(\text{La})$ in good agreement with experiment, but it predicted $z(\text{As}) \sim 0.139$, which is 0.011 off the experimental value, about 0.1 Å in length. However, Wien2K with PBE(GGA) XC functional gives an optimized $z(\text{As}) \sim 0.149$, which agrees well with experimental $z(\text{As})$. Similar results are found in the XFe_2As_2 family ($\text{X}=\text{Ba}, \text{Sr}, \text{Ca}$) too. It suggests that, GGA (PBE) XC functional optimizes the FeAs-based system much better than LDA (PW92) XC functional. And GGA should have better performance in dealing with the structure (including c/a , equilibrium volume and $z(\text{As})$) under pressure of this FeAs family. This is probably due to the layered structure of the FeAs family which results in large density gradient between layers, thus GGA has better description of the potential. But in the meantime, GGA (PBE) further overestimates the magnetic moment of Fe, which is already overestimated by LDA (PW92).

B. Effect of $z(\text{As})$ on the electronic structure of LaOFeAs

Then we studied how the electronic structure of LaOFeAs depends on the value of $z(\text{As})$. Table II shows the difference between the experimental $z(\text{As}) (\sim 0.150)$, the optimized $z(\text{As}) (\sim 0.139)$ and a middle value of 0.145 when using FPLO7 with PW92 XC functional: decreasing $z(\text{As})$ (reducing the Fe-As distance) rapidly reduces the differences in energy between

TABLE I: Calculated magnetic moment of Fe, the amounts of total energy per Fe lie below non-magnetic state of FM, Q_0 AFM and Q_M AFM states from FPLO7 and Wien2K with different XC functionals of LaOFeAs with experimental structure. Positive Δ EE means lower total energy than NM state.

code	XC	mag. mom. (μ_B)			Δ EE (meV/Fe)		
		Q_M	Q_0	FM	Q_M	Q_0	FM
FPLO7	PW92	1.87	1.72	0.00	87.2	24.6	0
	PZ	1.70	1.31	0.00	62.2	6.9	0
WIEN2k	PW92	1.74	1.52	0.13	136.9	78.9	0
	GGA	2.09	1.87	0.36	149.1	65.2	3.7
	PBE	2.12	1.91	0.37	158.1	70.2	4.5
0.1 e ⁻ doped	PW92	1.86	—	0.08	125.2	—	-0.5
0.1 e ⁻ doped	GGA	2.14	—	0.26	139.7	—	-0.1
0.1 e ⁻ doped	PBE	2.16	—	0.27	149.6	—	2.1

TABLE II: Calculated magnetic moment of Fe, total energy relative to the nonmagnetic (ferromagnetic) states of NM/FM, Q_0 AFM and Q_M AFM of LaOFeAs with $z(\text{As}) = 0.150$ (experimental), 0.145, and 0.139 (optimized) from FPLO7 with PW92 XC functional.

$z(\text{As})$	mag. mom. (μ_B)			Δ EE (meV/Fe)		Fe 3d occ.#	
	Q_M	Q_0	FM	FM- Q_M	Q_0 - Q_M	maj.	min.
0.150	1.87	1.72	0.002	87.2	62.6	4.32	2.45
0.145	1.70	1.41	0.000	60.5	54.0	4.24	2.55
0.139	1.48	0.01	0.000	34.6	34.6	4.15	2.68

the different magnetic orderings. At $z(\text{As}) = 0.145$, the magnetic moments of the Q_M and Q_0 states are reduced significantly in comparison with $z(\text{As}) = 0.150$, and the difference in energy has changed by around 20%, indicating important changes in the electronic structure upon moving the As atom. For $z(\text{As}) = 0.139$, the Q_0 AFM state has lost its moment (become the NM state), while the magnetic moment of the Q_M state has decreased even more,

with a changing rate of $6.8 \mu_B/\text{\AA}$, indicating strong magnetophonon coupling.⁸ Therefore, using the experimental or optimized value for the internal coordinate of As gives quite different results and might explain several of the discrepancies seen in the previously published works. In Figures 3 and 4, we present the corresponding band structures, total densities of

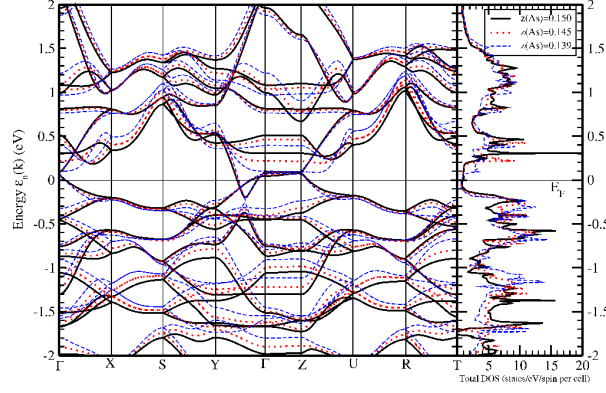


FIG. 3: The bandstructure and total DOS of Q_M LaOFeAs at ambient pressure computed for $z(\text{As})=0.150$, $z(\text{As})=0.145$, $z(\text{As})=0.139$.

states, and partial densities of states calculated for different values of $z(\text{As})$. Surprisingly, the band structure near E_F referred to the common Fermi level barely changes when $z(\text{As})$ decreases. Somewhat away from E_F , the bands below the Fermi level are pushed up in en-

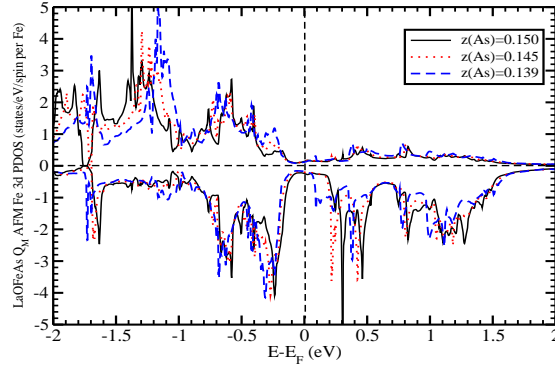


FIG. 4: Plot of LaOFeAs Q_M AFM Fe 3d PDOS at ambient pressure with $z(\text{As})=0.150$, $z(\text{As})=0.145$, $z(\text{As})=0.139$.

ergy when $z(\text{As})$ is decreased, while the effect of the Fe-As distance on the bands above ϵ_F is less obvious, since they are pushed up or down depending on the direction of the Brillouin zone. For instance, along $\Gamma - X$ and $\Gamma - Z$ they are pushed down, so that a decrease of the pseudogap is expected, as shown by Fig. 3. The peaks of the DOS just above Fermi level move toward it when $z(\text{As})$ is reduced, while the DOS below the Fermi level is quite robust with less changes. The important decrease of the magnetic moment of Fe when the Fe-As distance changes is understood by looking at the Fe-3d PDOS (Fig. 4) and the last column of table II. Although the number of Fe-3d electrons remains approximately constant, the number of spin up electron decreases, while the number of spin down electrons is increased when $z(\text{As})$ is reduced, which overall leads to a decrease of the magnetic moment.

C. Effect of virtual crystal doping on the electronic structure of LaOFeAs

Since superconductivity happens only in doped LaOFeAs, it is necessary to know how doping will affect the underlying electronic structure and the character of each magnetic state. Using the experimental lattice parameters, we performed virtual crystal doping calculations on LaOFeAs using Wien2K by changing the charge of O (doping with F) and La (doping with Ba, but simulating doping with Sr as well), and the corresponding number of valence electrons. The virtual crystal method is superior to a rigid band treatment because the change in carrier density is calculated self-consistently in the average potential of the alloy.

There is only a weak dependence of the calculated Fe magnetic moment on the electron doping level: 0.1 e^-/Fe doping enhances it from 2.12 μ_B to 2.16 μ_B (see Table I). However, electron doping reduces the total energy difference (compared to NM) in both Q_M AFM and FM states. The main effect of virtual crystal doping is to change the Fermi level position, in roughly a rigid band fashion (see the caption of Fig. 5 for more details). The band structures of 0.1, and 0.2 e^-/Fe doped LaOFeAs in the Q_M AFM phase show only small differences; the charge goes into states that are heavily Fe character and the small change in the Fe 3d site energy with respect to that of As 4p states is minor.

Notably, the virtual crystal approximation continues to give strong magnetic states,

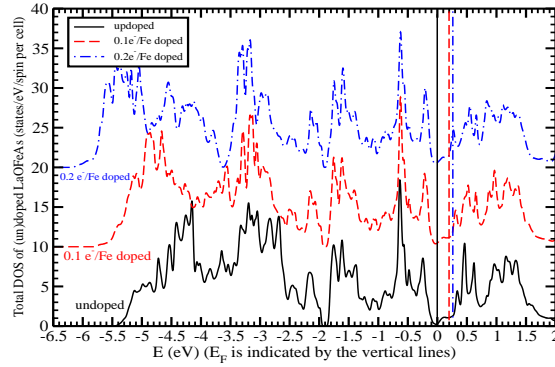


FIG. 5: Plots of undoped, 0.1 and 0.2 electron-doped LaOFeAs Q_M AFM total DOS (displaced upward consecutively by 10 units for clarity, obtained using the virtual crystal approximation. Referenced to that of the undoped compound, the Fermi levels of 0.1 and 0.2 electron-doped DOS are shifted up by 0.20 eV and 0.26 eV, respectively.

whereas doping is observed to degrade and finally kill magnetism and promote superconductivity. Thus the destruction of magnetism requires some large effect not considered here, such as strong dynamical spin fluctuations.

D. Electric field gradients

We have calculated the electric field gradients (EFG) of each atom in LaOFeAs, studying both the effects of doping and of magnetic order. The structure used for these calculations is $a=4.0355$ Å, $c=8.7393$ Å, $z(\text{La})=0.142$, $z(\text{As})=0.650$, and the PBE(GGA) XC functional was used in the Wien2K code. (PW92 (LDA) XC functional gives similar results and thus the results are not presented here.) Since the EFG is a traceless symmetric 3×3 matrix, only two of V_{xx} , V_{yy} , V_{zz} are independent. For cubic site symmetry, the EFG vanishes, hence the magnitude and sign of the EFG reflects the amount and character of anisotropy of the charge density. For the symmetries studied here, the off-diagonal components of the EFG tensor for all the four atoms are zero. For the Q_M AFM state, the V_{yz} component calculated separately for each spin for La and As is not zero, although the sum vanishes; the

spin decomposition gives information about the anisotropy of the spin density that is not available from measurements of the EFG.

As shown in Table III and Table IV, the EFGs of both Fe and As in NM and FM states are very similar and they are doping insensitive, except for Fe where the EFG is comparatively small (in tetrahedral symmetry, the EFG is identically zero). Due to the breaking of the x-y symmetry in the Q_M phase, V_{xx} is no longer equal to V_{yy} . In this case, the EFGs are quite different from those in the NM and FM states, which shows once more that the electronic structure in the Q_M AFM order differs strongly from the ones of the NM and FM orders. Also, while hole doping (on the La site) and electron doping (on the O site) significantly change the EFG of Fe, the EFG of As is less affected. Using nuclear quadrupolar resonance (NQR) measurement, Grafe *et al.*³² reported a quadrupole frequency $\nu_Q=10.9$ MHz and an asymmetry parameter $\eta=0.1$ of the As EFG in $\text{LaO}_{0.9}\text{F}_{0.1}\text{FeAs}$. This observation gives $V_{zz} \sim 3.00 \times 10^{21}$ V/m², which agrees reasonably well with our result of 2.6×10^{21} V/m² as shown in Table IV in the NM state. Upon 0.1 electron or 0.1 hole doping, the EFGs are modified in a similar way for As but differently for Fe.

E. Effect of pressure on the electronic structure of LaOFeAs

Applying pressure is often used as a way to probe how the resulting effect on the electronic structure impacts the superconducting critical temperature and other properties. A strong pressure effect was shown experimentally for the members of the LaOFeAs family^{9,10,33}, since for example $T_c = 43$ K could be reached under pressure for $\text{LaO}_{1-x}\text{F}_x\text{FeAs}$, in case of optimal doping⁹. To begin to understand such observations, it is necessary to determine how the electronic structure of the parent compound LaOFeAs is changed by pressure.

In Fig. 6, the magnetic moment of Fe in the Q_M AFM phase versus Fe-As distance is presented. Two different behaviours of the magnetic moment are observed. When $z(\text{As})$ is varied at constant volume (zero pressure), the decrease of the magnetic moment of Fe is parabolic. When pressure is applied and all internal positions are optimized (hence $z(\text{As})$ changes) the change is linear until the magnetic moment drops to zero. This linear behavior is followed also when the As height $z(\text{As})$ is shifted by 0.011 to compensate for the PW92

TABLE III: The EFG of Fe in LaOFeAs with NM, FM and Q_M AFM states at different doping levels from Wien2K with PBE(GGA) XC functional. The unit is 10^{21} V/m².

Fe		V_{xx}			V_{yy}		
	doping	up	dn	total	up	dn	total
NM	undoped	0.11	0.11	0.22	0.11	0.11	0.22
	0.1h (La)	0.21	0.21	0.42	0.21	0.21	0.42
	0.1e (La)	0.01	0.01	0.02	0.01	0.01	0.02
	0.1e (O)	0.09	0.09	0.18	0.09	0.09	0.18
FM	undoped	0.51	-0.30	0.21	0.51	-0.30	0.21
	0.1h (La)	0.05	0.39	0.44	0.05	0.39	0.44
	0.1e (La)	0.31	-0.21	0.10	0.31	-0.21	0.10
	0.1e (O)	0.31	-0.20	0.11	0.31	-0.20	0.11
Q_M	undoped	0.22	0.03	0.25	-1.11	0.54	-0.57
	0.1h (La)	0.60	-1.13	-0.43	-1.15	1.04	-0.11
	0.1e (La)	-0.55	1.00	0.45	-1.05	0.24	-0.81
	0.1e (O)	-0.54	1.01	0.47	-1.07	0.32	-0.75
	0.2e (O)	-0.82	1.17	0.35	-1.02	0.52	-0.50

(LDA) error mentioned above. Fig. 7 collects a number of results: the effect of pressure on the c/a ratio, the Fe-As distance, the total energy, the difference in energy between NM and Q_M states, and the magnetic moment on Fe. Under pressure, the c/a ratio, the Fe-As distance, and the magnetic moment of the Q_M AFM state drop linearly when volume is reduced. The PW92(LDA) predicts an equilibrium volume of $0.925 V_0$; and the total energy differences between NM and Q_M AFM state gradually drops to zero at $0.78 V_0$.

The effect of pressure on the band structure is shown in Fig. 8. While the bands change positions under pressure, in the corresponding DOS (right panel of Fig. 8), the first peak above E_F is moved towards the Fermi level when pressure is applied, but the DOS from -0.1 eV to E_F is left almost unchanged by pressure. Therefore pressure should induces important changes in the superconducting properties of electron-doped LaOFeAs, while they should be

TABLE IV: The EFG of As in LaOFeAs with NM, FM and Q_M AFM states at different doping levels from Wien2K with PBE(GGA) XC functional. The unit is 10^{21} V/m².

As		V_{xx}			V_{yy}		
	doping	up	dn	total	up	dn	total
NM	undoped	0.69	0.69	1.38	0.69	0.69	1.38
	0.1h (La)	0.70	0.70	1.40	0.70	0.70	1.40
	0.1e (La)	0.65	0.65	1.31	0.65	0.65	1.31
	0.1e (O)	0.66	0.66	1.32	0.66	0.66	1.32
FM	undoped	0.55	0.81	1.36	0.55	0.81	1.36
	0.1h (La)	0.58	0.68	1.26	0.58	0.68	1.26
	0.1e (La)	0.56	0.74	1.30	0.56	0.74	1.30
	0.1e (O)	0.58	0.75	1.23	0.58	0.75	1.23
Q_M	undoped	-0.40	-0.40	-0.80	0.77	0.77	1.54
	0.1h (La)	-0.42	-0.42	-0.84	0.68	0.68	1.36
	0.1e (La)	-0.41	-0.41	-0.82	0.89	0.89	1.78
	0.1e (O)	-0.40	-0.40	-0.80	0.91	0.91	1.82
	0.2e (O)	-0.29	-0.29	-0.58	1.03	1.03	2.06

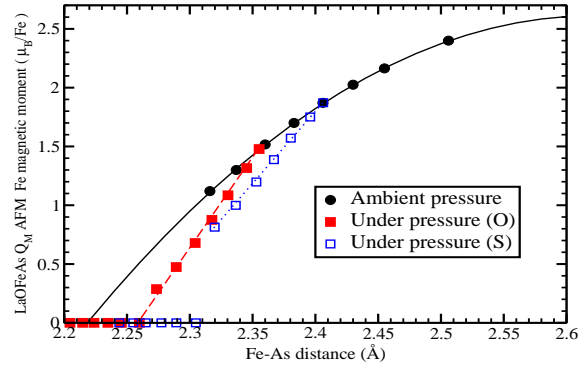


FIG. 6: Plot of the magnetic moment of Fe atom in the Q_M AFM state of LaOFeAs as a function of the Fe-As distance, both at ambient pressure and under pressure.

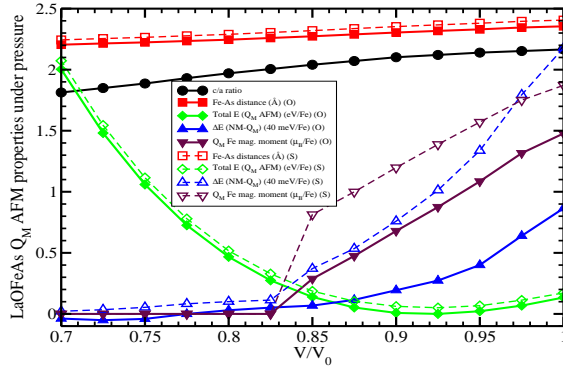


FIG. 7: Plot of the optimized c/a ratio, the Fe-As distances (Å), the total energy of the Q_M AFM state (eV), the total energy differences between NM and Q_M AFM state (EE(NM)-EE(Q_M AFM) (40 meV/Fe), the magnetic moment (μ_B) of the Q_M AFM states as a function of V/V_0 .

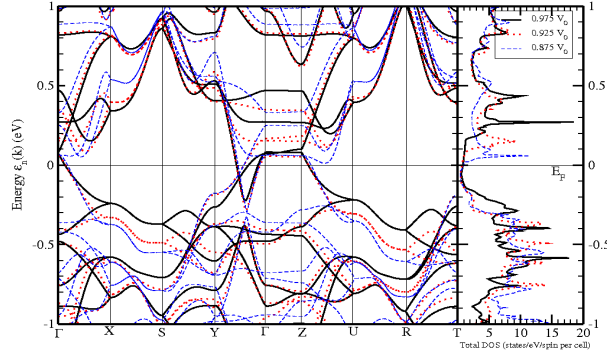


FIG. 8: The bandstructure and total DOS of Q_M LaOFeAs computed for $0.975V_0$, $0.925 V_0$ and $0.875 V_0$. $z(\text{As})$ has been shifted.

less important for hole-doped LaOFeAs.

The Fermi surface of Q_M LaOFeAs computed for different values of the volume is presented in Fig. 9. The first sheet is an almost perfect cylinder along the $\Gamma - Z$ line, while the second sheet is made of two ellipsoidal cylinders with some k_z bending. They appear to be very similar to the FS computed at ambient pressure⁸. The pressure has almost no effect on the first sheet, but it enhances the distortion of the second sheet.

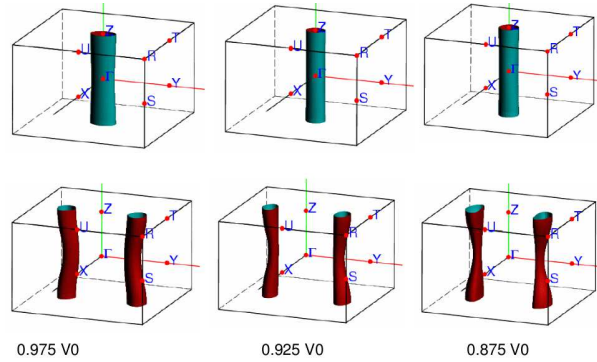


FIG. 9: The Fermi surface of Q_M LaOFeAs computed for $0.975V_0$, $0.925 V_0$ and $0.875 V_0$. $z(\text{As})$ has been shifted.

V. INVESTIGATION OF THE STRUCTURAL DISTORTION AND OF THE (π, π, π) MAGNETIC ORDER

Magnetic $\vec{q} = (\pi, \pi, \pi)$ magnetic order in stoichiometric LaOFeAs (with magnetic cell being $\sqrt{2} \times \sqrt{2} \times 2$ the crystallographic cell) was reported first by de la Cruz et al.² using inelastic neutron scattering. Ordering takes place at $T_N = 135 - 140$ K and is preceded in temperature by a structural distortion occurring around 155 K. These transitions have since been confirmed by other groups.³ A similar structural distortion was found for NdOFeAs³⁴, showing that the temperature of the structural phase transition in this case is reduced by about 20 K in comparison with LaOFeAs. These phase transitions have been revisited³⁵ using various experimental tools (heat capacity, ultrasound spectroscopy etc..). Although the magnetic ordering of FeAs layers along the c axis is less likely to be crucial for the mechanism of superconductivity since the involved scale of energy is expected to be very weak in comparison with the intralayer ordering, its study is necessary to understand the complete system. For the same reason, and even if there are strong indications that it does not happen in the case of F-doped LaOFeAs, it is interesting to see whether the structural distortion of pure LaOFeAs can be reproduced by ab-initio calculations, and what the corresponding electronic structure looks like. The results we present in this section were obtained using the VASP code with the PBE(GGA) functional²⁰.

A. $(\pi, \pi, 0)$ structural order

The structural transformation^{2,3} changes the $\sqrt{2} \times \sqrt{2}$ cell (with four iron atoms; full lines in Fig. 2) from tetragonal (space group $P4/nmm$) to orthorhombic (space group $Cmma$) or equivalently for the primitive cell (with two iron atoms; dashed lines in Fig. 2) from tetragonal (space group $P4/nmm$) to monoclinic (space group $P112/n$). To simplify our study, the cell doubling along the c axis due to magnetic ordering is neglected for this study, i.e. we consider only the $(\pi\pi 0)$ order. We have performed a relaxation (shape of the cell as well as atom positions) of LaOFeAs for different volumes, the results being presented in Fig. 10. The calculated equilibrium lattice parameters as well as the internal atomic positions are reported in Table V, together with available experimental data. The overall agreement is satisfactory, the length of the a and b lattice cell vectors being slightly overestimated by our calculations, while the value of c is slightly underestimated. The value of $|\delta|$ (the monoclinic distortion angle) is overestimated by our calculations, but the very small distortion and very small energy difference makes this difference understandable. The important point is that ab-initio calculations are indeed able to reproduce the structural instability of LaOFeAs.

As for the atom positions within the cell, the agreement is good for the positions of La, O, and Fe but is less satisfying for the internal position $z(\text{As})$ of arsenic. The difficulty concerning the position of As has been reported by us previously⁸ and is related to the strong magnetophonon coupling that occurs in this compound. In Fig. 10, we present the corresponding lattice parameters (upper plot); magnetic moment (middle plot); and internal coordinate of As (z_{As}) (lower plot), versus volume for LaOFeAs. The range of pressure covered goes roughly from -2.5 GPa to 2.5 GPa. By fitting the E-V data (not shown here) to a Birch-Murnaghan equation of state (EOS), we find LaOFeAs to have a bulk modulus of $B_0 = 75$ GPa and a bulk modulus derivative $B'_0 = 4.1$. Also, from the upper plot of Fig. 10, we predict that LaOFeAs is more compressible along the c axis than along the a and b axes, a common characteristic of layered materials.

More important is the dependence of the magnetic moment on the volume (middle plot of Fig. 10). This dependence has two origins: the first one is the usual dependence of the magnetic moments on the volume change, but in LaOFeAs, the magnetic moment on Fe

TABLE V: Left and middle columns: the structure parameters of LaOFeAs in its low-temperature phase as obtained from x-ray³ and neutron² studies, as reported by Yildirim³⁶. Right column: results from calculations obtained after a full relaxation of a $\sqrt{2} \times \sqrt{2}$ cell with a $(\pi\pi 0)$ magnetic order. a , b , and c are the lattice parameters, $|\delta|$ is the monoclinic distortion angle of the primitive cell, and La(z), As(z), O(z), and Fe(z) are the internal coordinate of the corresponding atom.

	X-ray (120 K)		Neutron (4K)	Calcs.
	$\sqrt{2} \times \sqrt{2}$	Primitive	Primitive	$\sqrt{2} \times \sqrt{2}$
a	5.68262 Å	4.02806 Å	4.0275 Å	5.69 Å
b	5.71043 Å	4.02806 Å	4.0275 Å	5.76 Å
c	8.71964 Å	8.71964 Å	8.7262 Å	8.70 Å
$ \delta $	0.2797°		0.279°	0.69°
La(z)	0.14171		0.1426	0.1418
As(z)	0.65129		0.6499	0.6451
O(z)	0		-0.0057	0.0
Fe(z)	0.5		0.5006	0.5

is known⁸ to be strongly dependent on the internal coordinate of As which changes with applied pressure (lower plot of Fig. 10).

The structural distortion has been addressed by Yildirim,^{30,36} who approached the question differently and obtained different results. While our value of the Fe moment is close to that for the undistorted structure as would be expected, the moment reported by Yildirim is $0.48 \mu_B$ per Fe atom. We checked carefully the possible existence of such a magnetic solution, but our calculations appears to be robust, with the magnetic moment of Fe being around $2 \mu_B$. As a result of the different magnetic moment, his computed DOS (see Fig. 5 in Ref. 30) also is different. Together with an experimental study, Nomura et al.³ reported ab-initio calculations on LaOFeAs for both the tetragonal and orthorhombic structures, and found almost vanishing magnetic moments, which correspond to a non-magnetic ground-state. In

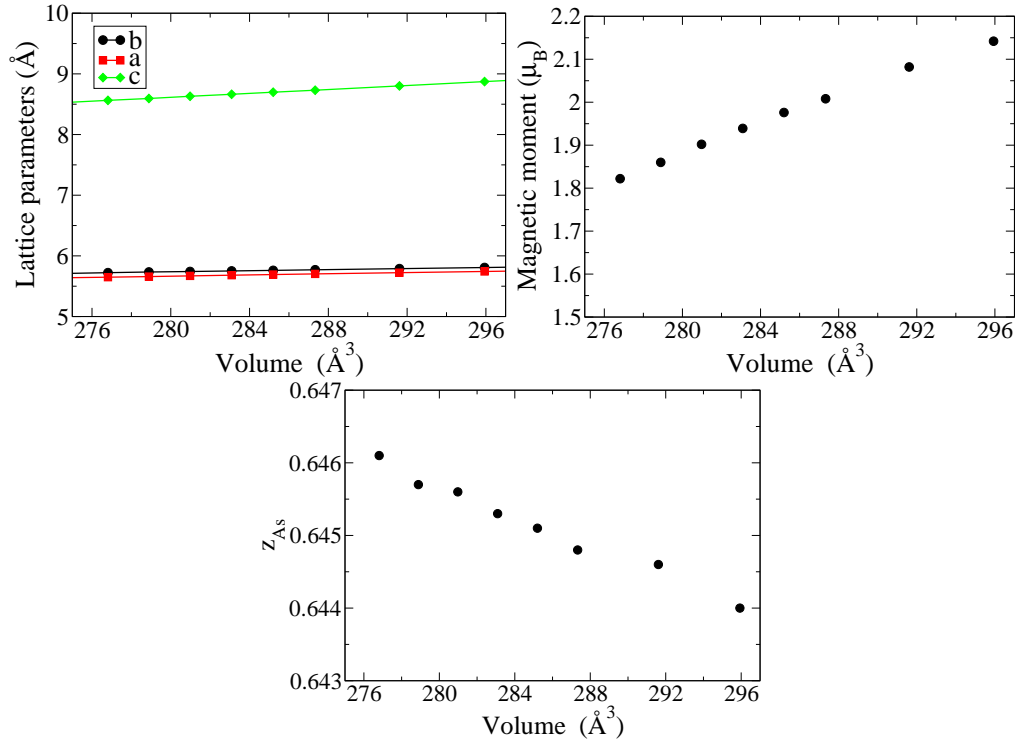


FIG. 10: Upper plot: Lattice parameters versus volume. Middle plot: magnetic moment versus volume. Lower plot: z_{As} versus volume.

our case, such a state is higher in energy by about 140 meV per Fe atom for the fully relaxed structure, and therefore can safely be ruled out as being the true ground-state of LaOFeAs. The differences in calculated values that we have noted reflect an unusual sensitivity to details (structure, method, XC functional).

B. (π, π, π) magnetic order

We turn now to the investigation of LaOFeAs taking into account both the true (π, π, π) magnetic order and the structural distortion. In this case, we have used the experimental structural data provided by de la Cruz et al.². As in the case of the $(\pi, \pi, 0)$ order, there are two possible magnetically ordered states. Only one gives the (π, π, π) order to be the ground state versus the $(\pi, \pi, 0)$ order, and by only few meV per Fe atom. This small energy difference is near the limit of precision of our calculations, but appears to confirm the sign

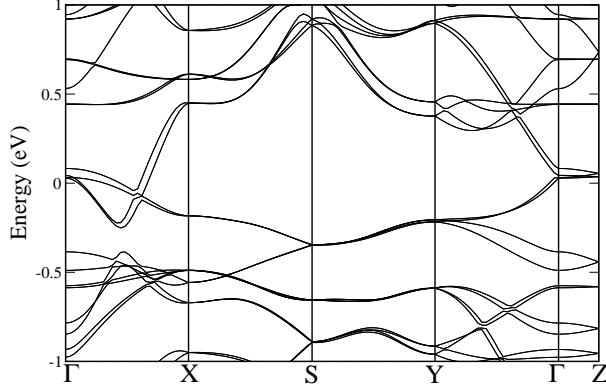


FIG. 11: The bandstructure of LaOFeAs along high-symmetry directions in the case of a $(\pi\pi\pi)$ magnetic order for the distorted (orthorhombic) $\sqrt{2} \times \sqrt{2} \times 2$ cell. The high symmetry points are defined as Γ (0,0,0); X (0.5,0,0); S (0.5,0.5,0); Y (0,0.5,0); and Z (0,0,0.5), in terms of reciprocal lattice vectors.

of the very weak magnetic interaction along the c layers.

The corresponding band structure is shown in Fig. 11. Due to the doubling of the cell along the c axis, there are now four bands crossing the Fermi level (see Fig. 3 of Ref. 8). Along S-Y there are tiny splittings around -0.25 and -0.6 eV as well as along Γ -X and Γ -Y, indicating the magnitude of interlayer coupling. In particular, the splitting is particularly large for one pair of bands just above E_F at Γ . Along X-S-Y, the bands nearest the Fermi level are hardly split at all. Overall, the band structure retains the essential features noticed before⁸, namely a pseudogap separating bonding and antibonding states over much of the zone, together with dispersive bands crossing the Fermi level along only one of the two in-plane directions ($\Gamma - X$, with our choice of axes).

The total and partial densities of states are very similar to the ones in the case of a $(\pi\pi 0)$ magnetic order and won't be shown here; but we notice that the rough electron/hole symmetry in view of the study of doped (superconducting) materials is preserved. Also, our calculated Fermi surface (not shown here), made of four sheets, is very similar to the one presented previously⁸ for the $(\pi, \pi, 0)$ order and folded back along k_z : it has two sheets along the $\Gamma - Z$ direction which are almost perfectly cylindrical, while the two other sheets are more distorted, but still showing a strong two-dimensional character.

VI. ROLE OF THE PNICTOGEN ATOM

As mentioned at the beginning of Section I of this paper, LaOFeAs and LaOFeP are isostructural and isovalent, but they have quite different properties: LaOFeAs is Q_M AFM ordered below $T_N=150$ K and not superconducting, while LaOFeP is a $T_c=2.5$ K superconductor¹ without magnetic order. Also, they have completely different response to doping: either electron or hole doping will destroy the Q_M AFM ordering in LaOFeAs and make it superconducting with T_c over 26 K⁴ (43 K under pressure⁹), while in LaOFeP, doping changes the critical temperature less significantly to only 9 K¹. A deeper understanding of the differences of the electronic structure of these two compounds can provide insight into the competition between magnetic ordering and superconductivity. For similar reasons, the related compounds LaOFeN and LaOFeSb (although not studied experimentally yet) are potentially of high interest, so we also provide predictions for their electronic structure.

Table VI displays the experimental structure parameters for LaOFeP¹ and LaOFeAs⁴ as well as the predicted structure for LaOFeN and LaOFeSb after optimization (see below for calculation details). As a result of the increasing size of the pnictogen atom, the Fe-Pn length changes. In particular, the Fe-Pn distance is consistent with the sum of the covalent radii of Fe and Pn, which reflects the covalent bonding nature between Fe and Pn atoms in this family. The slight increase of the La-O distance through the series is just a size effect related to the expansion of the volume .

The values of the Fe magnetic moment for LaOFePn with FM/NM, Q_0 AFM, Q_M AFM states, and their total energy differences are presented in Table VII. Apart from LaOFeP, all the members of the LaOFePn family studied here have a large Fe magnetic moment in the Q_M AFM state, the corresponding total energy being significantly lower than the ones corresponding to FM/NM state.

A. LaOFeP

LaOFeP was the first member of the iron-oxypnictide family to be reported to be superconducting¹. The corresponding electronic structure was studied by Lebègue using ab-

Pn	a (Å)	c (Å)	c/a	z(La)	z(Pn)	La-O	Fe-Pn	Sum
N	3.6951	8.0802	2.187	0.170	0.109	2.302	2.047	2.00
P	3.9636	8.5122	2.148	0.149	0.134	2.352	2.286	2.31
As	4.0355	8.7393	2.166	0.142	0.151	2.369	2.411	2.44
Sb	4.1626	9.3471	2.246	0.127	0.171	2.396	2.624	2.62

TABLE VI: Structural parameters of LaOFePn (Pn = N, P, As, or Sb), as obtained experimentally for LaOFeP¹ and LaOFeAs⁴ or from our calculations for LaOFeN and LaOFeSb. Length units are in Å, $z(\text{La})$ and $z(\text{Pn})$ are the internal coordinate of the lanthanum atom and the pnictide atom, and “Sum” means the sum of Fe covalent radius and the Pn covalent radius, which is quite close to the calculated value in all cases.

Pn	mag. mom. (μ_B)			Δ EE (meV/Fe)	
	Q_M	Q_0	FM	FM- Q_M	Q_0 - Q_M
N	1.63	0.80	0.027	41.0	40.0
P	0.56	—	0.087	1.6	—
As	1.87	1.72	0.002	87.2	62.6
Sb	2.47	2.43	0.000	293.8	82.4

TABLE VII: Calculated magnetic moment of Fe, total energy relative to the nonmagnetic (ferromagnetic) states of Q_0 AFM, and Q_M AFM states of LaOFePn from FPLO7 with PW92 XC functional.

initio calculations⁶, but considering only a non-magnetic ground-state. Since then LaOFeP has been studied using various experimental tools: by using photoemission^{37,38,39}, it was shown that the Fe 3d electrons are itinerant, and that there is no pseudogap in LaOFeP. Also, magnetic measurements revealed^{40,41} that LaOFeP is a paramagnet, while electron-loss spectroscopy⁴² implied a significant La-P hybridization. The absence of long-range order in LaOFeP was confirmed by Mössbauer spectroscopy⁴³ and it was proposed that LaOFeP and doped LaOFeAs could have different mechanisms to drive the superconductivity in these compounds. Also, further theoretical studies were performed^{39,40,42} but without studying all

the possible magnetic states.

In our calculations, we find that for FM order Fe has a weak magnetic moment of about $0.09 \mu_B$, with a total energy very close to the NM one; this result is much like what is found in LaOFeAs. A remarkable difference is that the Q_0 AFM state cannot be obtained. However, we found the Q_M AFM state to be the lowest in energy, but only by about 1.6 meV/Fe, which is about two orders of magnitude less than in LaOFeAs. LaOFeP, therefore, presents the situation where all of the three possible magnetic states are all very close in energy to the nonmagnetic state, in contrast with LaOFeAs for which the Q_M AFM order was clearly the ground state. Thus LaOFeP is surely near magnetic quantum criticality.

The band structure of Q_M AFM LaOFeP is displayed in Fig. 12 together with total DOS for both Q_M AFM and NM states. The band structure of Q_M AFM LaOFeP is quite different from that of LaOFeAs with the same Q_M order, with the most significant differences along Γ -X, Γ -Y and Γ -Z lines. The difference is because the breaking of the $x - y$ symmetry is much smaller in the Q_M AFM LaOFeP compared to LaOFeAs, because the calculated Fe moment is only $0.56 \mu_B$ in LaOFeP (it is $1.87 \mu_B$ in LaOFeAs with the same calculational method). The corresponding DOS is also different from that of LaOFeAs: there is structure within the pseudogap around Fermi level in LaOFeP (See Fig. 12). The difference in total DOS at E_F is significant: it is only 0.2 states/eV/spin per Fe for LaOFeAs, but it is 0.6 states/eV/spin per Fe for LaOFeP. In the NM state of LaOFeP, it is even larger with 1.6 states/eV/spin per Fe. The DOS of Q_M AFM LaOFeP is fairly flat from the Fermi level (set to 0.0 eV) to 0.6 eV, so that electron doping of LaOFeP will increase the Fermi level, but will hardly change $N(E_F)$ (in a rigid band picture).

An important consequence is that there will be no expected enhancement of T_C coming from $N(E_F)$ upon electron doping. In order to see a significant increase of $N(E_F)$ in Q_M AFM LaOFeP, an electron doping level of at least $1.2 e^-/\text{Fe}$ is required, which seems unrealistically large based on the current experimental information. This conclusion remains valid in the case of NM LaOFeP, since apart from a peak around Fermi level, the DOS is about the same as for the Q_M AFM state. Again, the behavior is quite different from the one of Q_M AFM LaOFeAs: $0.1 e^-/\text{Fe}$ doping will increase its $N(E_F)$ by a factor of 6: from 0.2 states/eV/spin

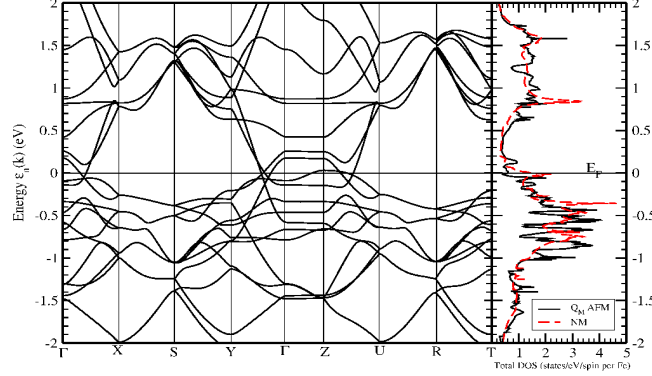


FIG. 12: Plot of LaOFeP band structure in Q_M AFM state and total DOS in both Q_M AFM and NM states at ambient conditions with experimental lattice parameters.

per Fe to 1.2 states/eV/spin per Fe.

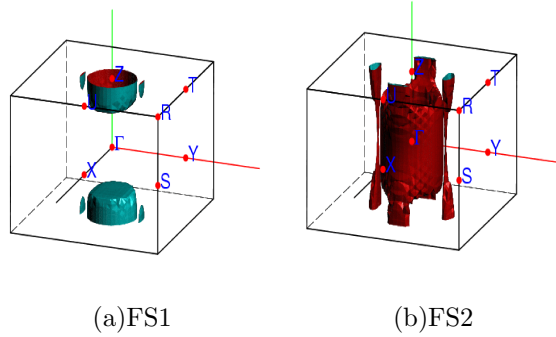


FIG. 13: Fermi surface of Q_M AFM LaOFeP, showing the very strong differences compared to LaOFeAs.

The Fermi surface of Q_M AFM LaOFeP is shown in Fig. 13. Compared to the Fermi surface of Q_M AFM LaOFeAs presented earlier by Yin *et al.*⁸, the piece enclosing the Γ -Z line (containing holes) increases in size and its $x - y$ cross section becomes more circular rather than elliptic. There is another piece (absent in LaOFeAs) also enclosing the Γ -Z line with the same shape but larger in size and containing electrons instead of holes. The two symmetric electron-type pieces of Fermi surface lying along Γ -Y direction in LaOFeAs reduces a lot in size in LaOFeP but it has two additional similar pieces lying along Γ -X direction. In LaOFeP, it has one more hole-type piece of Fermi surface surround Z point, which is a small cylinder. It is, understandably, quite different from the Fermi surface of

V/V_0	a (Å)	c (Å)	c/a	$z(\text{La})$	$z(\text{Sb})$
1.000	4.092	8.500	2.077	0.137	0.165
1.050	4.118	8.812	2.140	0.133	0.163
1.100	4.141	9.131	2.205	0.129	0.161
1.125	4.155	9.274	2.232	0.128	0.160
1.138	4.163	9.347	2.245	0.127	0.160
1.150	4.169	9.418	2.259	0.126	0.159

TABLE VIII: Optimized structure parameters for LaOFeSb at several volumes. The accuracy for c/a is within 0.3%, and within 0.8% for $z(\text{La})$ and $z(\text{Sb})$.

NM LaOFeP presented earlier⁶.

Therefore, while they are isostructural and significantly covalent, LaOFeP and LaOFeAs present quite important differences in their respective electronic structures. These differences must form the underpinning of any explanation of why LaOFeP is superconducting with a T_c which is almost electron-doping independent, while pure LaOFeAs is not superconducting and becomes so only upon doping.

B. LaOFeSb

Since the experimental crystal structure of LaOFeSb is not reported yet, we conducted calculations to obtain the structure. The procedure we used is the following: starting from the experimental volume V_0 of LaOFeAs (but with As replaced by Sb), we first optimized c/a , $z(\text{La})$ and $z(\text{Sb})$. Then we chose a higher volume and again optimized the parameters, finally finding the volume that has the lowest total energy. Using this scheme, the optimized volume is 1.046 V_0 while for LaOFeAs the equilibrium volume is about 0.919 V_0 . Assuming that PW92 overbinds equally for LaOFeSb as for LaOFeAs, the experimental equilibrium volume for LaOFeSb should be $1.046/0.919=1.138 V_0$. Therefore, we performed calculations for a range of volume from $V = V_0$ to $V = 1.150 V_0$, the corresponding structural parameters being presented in Table VIII.

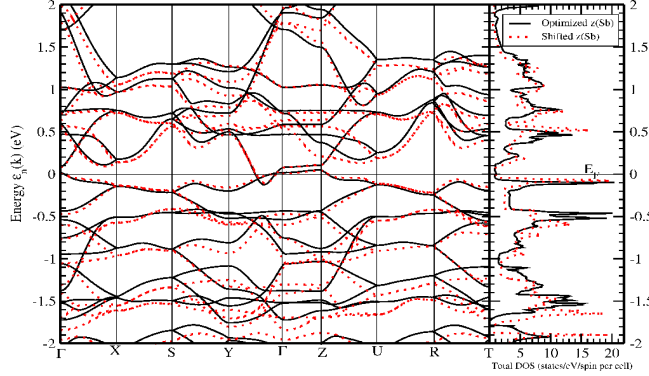


FIG. 14: Plot of Q_M AFM LaOFeSb band structure and total DOS at $1.138 V_0$ with both optimized and shifted $z(\text{Sb})$.

Since for LaOFeAs in the Q_M AFM phase PW92 underestimated $z(\text{As})$ by 0.011 at its experimental volume, we corrected $z(\text{Sb})$ by adding 0.011 to the optimized $z(\text{Sb})$ (we refer to this position at the “shifted $z(\text{Sb})$ ”). Both for the NM and Q_M AFM case, there are very small differences near E_F between the optimized $z(\text{As})$ and shifted $z(\text{As})$ in the band structure and DOS, as seen in Fig 14. However, shifting $z(\text{Sb})$ induces important changes in the energy differences between NM and Q_M AFM states, as shown in Table IX. Also, the magnetic moment of Fe, and the energy differences among NM/FM, Q_0 AFM and Q_M AFM are strongly dependent on the volume. With decreasing volume, the difference in energy between the different magnetic states decreases quickly.

At $1.138 V_0$, the inferred equilibrium volume of LaOFeSb, the properties of NM/FM, Q_0 AFM, and Q_M AFM are very similar to the ones of LaOFeAs at its experimental volume. Thus from these results we expect that doped LaOFeSb should have similar properties (viz, value of T_c) as LaOFeAs.

C. LaOFeN

The structure of LaOFeN is also not reported experimentally. In order to obtain it, the same procedure as for LaOFeSb was used. The lowest total energy is at $0.762 V_0'$ (here V_0' is the experimental volume of LaOFeP.). Again assuming PW92 makes a similar error as it makes in LaOFeAs, we estimate its equilibrium volume to be close to $0.825 V_0'$. At 0.825

V/V ₀	mag. mom. (μ_B)			Δ EE (meV/Fe)	
	Q _M	Q ₀	FM	FM-Q _M	Q ₀ -Q _M
1.000	1.58	1.12	0.36	60.1	60.1
1.050	1.87	1.74	0.44	95.6	68.0
1.100	2.09	2.00	0.00	147.6	70.7
1.125	2.17	2.10	0.00	172.6	71.8
1.138	2.23	2.16	0.00	190.6	72.5
1.150	2.26	2.19	0.00	199.0	72.0
1.050	2.17	2.08	0.72	158.1	78.0
1.100	2.35	2.00	0.00	223.8	80.8
1.125	2.42	2.37	0.00	271.6	81.8
1.138	2.47	2.42	0.00	293.8	82.4
1.150	2.49	2.45	0.00	287.6	82.1

TABLE IX: Calculated magnetic moment of Fe, total energy relative to the nonmagnetic (ferromagnetic) states of Q₀ AFM and Q_M AFM with the optimized structure of LaOFeSb at several volumes from FPLO7 with PW92 XC functional. Upper part: z(Sb) is optimized. Lower part: z(Sb) is optimized and shifted.

V₀' and for larger volume, the total energy of the Q_M AFM state is well below that of the FM/NM state (see Table X). Therefore, LaOFeN, if it exists, should be in the Q_M AFM ordered state at low temperature, which is similar to LaOFeAs and LaOFeSb.

Compared to the other LaOFePn compounds, LaOFeN is even closer to being a semimetal when the volume is equal to 0.825 V₀', and it becomes a small gap insulator at 0.850 V₀' and a higher carrier density metal at 0.800 V₀' (see Fig. 15). The DOS for 0.825 V₀' shows a pseudogap around E_F, but the DOS is somewhat less flat than it is for LaOFeAs.

When LaOFeN is calculated to be insulating (for volumes larger than 0.825 V₀'), the gap can be taken to *define* a distinction between bonding (occupied) and antibonding (unoccupied) states. The appearance of this gap in LaOFeN is quite surprising: although there is clear separation of valence and conduction bands over most of the zones for LaOFeAs, there

V/V_0'	mag. mom. (μ_B)			Δ EE (meV/Fe)	
	Q_M	Q_0	NM/FM	NM/FM- Q_M	Q_0 - Q_M
0.900	2.21	1.69	1.64	209.8	135.9
0.875	2.06	1.51	0.03	114.9	99.2
0.850	1.88	1.14	0.03	74.3	68.1
0.825	1.63	0.80	0.03	41.0	40.0
0.800	1.26	—	0.00	18.4	—
0.787	1.08	—	0.00	11.3	—
0.775	0.90	—	0.00	7.0	—
0.762	0.00	—	0.00	1.3	—
0.750	0.00	—	0.00	1.4	—
0.725	0.00	—	0.00	1.2	—
0.700	0.00	—	0.00	0.9	—

TABLE X: Calculated magnetic moment of Fe in LaOFeN, total energy relative to the nonmagnetic (ferromagnetic) states of Q_0 AFM and Q_M AFM with the optimized structure at several volumes, but shifted $z(N)$ up by 0.011, as a compensation PW92 does to LaOFeAs, where PW92 underestimates $z(As)$ by 0.011.

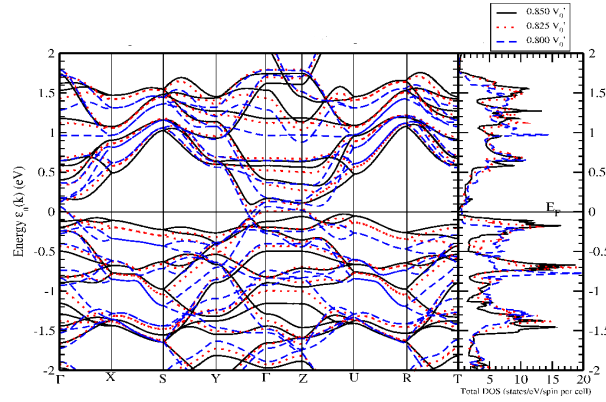


FIG. 15: Plot of LaOFeN Q_M AFM band structure and total DOS at $0.850V_0'$, $0.825 V_0'$ and $0.800 V_0'$ with shifted $z(N)$.

is no way to ascribe the small FSs to simple overlapping valence and conduction bands: in LaOFeAs and LaOFeSb, the bonding and antibonding bands are never completely separated from each other. In LaOFeN this separation finally becomes apparent, as an actual bandgap does appear.

VII. ROLE OF THE RARE EARTH ATOM IN REOFEAS

After LaOFeAs was discovered, after appropriate variation of the carrier concentration, to be superconducting at 26 K, much substitution on the rare earth (R) site has been done, with impressive increases in the critical temperature. Since all are evidently trivalent and donate three valence electrons to the FeAs layer, it becomes important to uncover the influence of the R atom: is it some aspect of the chemistry, which does differ among the rare earths? is it an effect of size? or can there be some other subtle effect?

Table XI is a collection of the lattice constants a and c , volume V of the primitive cell, T_c onset of ROFeAs reported from experiment.^{44,45,46,47} Both lattice constants, hence the volume, decrease monotonically as the atomic number increases, but T_c increases only from La to Gd, whereupon drops for heavier rare earths. Since we have found that small details affect the electronic and magnetic structure – especially $z(\text{As})$ – it is reasonable to assess the size effect. We have performed calculations on Ce, Nd and Gd, using LSDA+U with $U=7.0$ eV and $J=1$ eV applied to the R atom to occupy the $4f$ shell appropriately and keep the $4f$ states away from the Fermi level. Our results indicate that all have very similar DOS and band structure with LaOFeAs. To investigate further, we checked GdOFeAs using the crystal structure of LaOFeAs. The resulting band structure and DOS are almost identical to the original results for Gd, thus there seems to be no appreciable effect of the differing chemistries of Gd and La. This negative result supports the idea that the size difference may be dominant, though seemingly small. The difference in size (hence a , c , and the internal coordinates) influences not only the band structure and DOS, but also the magnetic properties. Fixed spin moment calculations in the FM state gives the lowest total energy at $0.2 \mu_B/\text{Fe}$ in LaOFeAs, and $0.5 \mu_B/\text{Fe}$ in both GdOFeAs and La-replaced GdOFeAs.

TABLE XI: Collection of the lattice constants a (\AA) and c (\AA), volume V (\AA^3) of the primitive cell, T_c onset s (onset, middle, and zero, in K) of ReOFeAs reported from experiments.

element	Z	$a(\text{\AA})$	$c(\text{\AA})$	$V(\text{\AA}^3)$	$T_{C,onset}$ (K)
La	57	4.033	8.739	142.14	31.2
Ce	58	3.998	8.652	138.29	46.5
Pr	59	3.985	8.595	136.49	51.3
Nd	60	3.965	8.572	134.76	53.5
Sm	62	3.933	8.495	131.40	55.0
Gd	64	3.915	8.447	129.47	56.3
Tb	65	3.899	8.403	127.74	52
Dy	66	3.843	8.284	122.30	45.3

VIII. SUMMARY

We have investigated in some detail the electronic structure and magnetic properties of the LaOFeAs class of novel superconductors using ab-initio methods. The effects of the Fe-As distance, of doping, and of pressure, as well as calculations of the EFGs have been reported. It was found that (approximate) electron-hole symmetry versus doping, and strong magnetophonon coupling are primary characteristics of the LaOFeAs system, and are two of the ingredients that need to be understood to proceed toward the discovery the mechanism of superconducting pairing. We studied effects of the structural distortion and of the (π, π, π) magnetic order, finding that experiments can be reproduced fairly well by our calculations. Finally, the related materials LaOFeP, LaOFeSb, and LaOFeN were investigated and their properties compared to those of LaOFeAs. From these comparisons, it appears that LaOFeP is significantly different from the other materials studied here; this difference might explain why, at stoichiometry, LaOFeP is superconducting while LaOFeAs is antiferromagnetic. Also, in view of their similarities with LaOFeAs, either pure or doped LaOFeSb and LaOFeN are potential candidates as superconductors.

IX. ACKNOWLEDGMENTS

We acknowledge financial support from ANR PNANO grant N^O ANR-06-NANO-053-02 and N^O ANR-BLAN07-1-186138 (S.L.) and from DOE Grant DE-FG03-01ER45876 (W.E.P.). W.E.P. is happy to acknowledge a grant from the France Berkeley Fund that enabled the initiation of this project.

-
- ¹ Y. Kamihara, *et al.*, J. Am. Chem. Soc. **128**, 10012 (2006).
² C. de la Cruz, *et al.*, Nature **453**, 899 (2008).
³ T. Nomura, *et al.*, (2008), arXiv/0804.3569.
⁴ Y. Kamihara, T. Watanabe, M. Hirano, and H. Hosono, J. Am. Chem. Soc. **130**, 3296 (2008).
⁵ Z.-A. Ren, *et al.* (2008), arXiv/0804.2053.
⁶ S. Lebègue, Phys. Rev. B **75**, 035110 (2007).
⁷ D. J. Singh and M.-H. Du, Phys. Rev. Lett. **100**, 237003 (2008).
⁸ Z. P. Yin, *et al.*, Phys. Rev. Lett. **101**, 047001 (2008).
⁹ H. Takahashi, *et al.*, Nature **453**, 376 (2008).
¹⁰ W. Lu, *et al.*, New Journal of Physics **10**, 063026 (2008).
¹¹ B. I. Zimmer, *et al.*, J. Alloy Comp. **229**, 238 (1995).
¹² P. Quebe, L. J. Terbuchte, and W. Jeitschko, J. Alloy Comp. **302**, 70 (2000).
¹³ P. Hohenberg and W. Kohn, Phys. Rev. **136**, B864 (1964).
¹⁴ W. Kohn and L. Sham, Phys. Rev. **140**, A1133 (1965).
¹⁵ K. Koepernik and H. Eschrig, Phys. Rev. B **59**, 1743 (1999).
¹⁶ K. Koepernik, B. Velicky, R. Hayn, and H. Eschrig, Phys. Rev. B **55**, 5717 (1997).
¹⁷ P. Blaha, K. Schwarz, G. K. H. Madsen, D. Kvasnicka, and J. Luitz, WIEN2k,(K. Schwarz, Techn. Univ. Wien, Austria) (2001).
¹⁸ J. P. Perdew and Y. Wang, Phys. Rev. B **45**, 13244 (1992).
¹⁹ J. Perdew, and A. Zunger, Phys. Rev. B **23**, 5048 (1981).
²⁰ J. Perdew, K. Burke, and M. Ernzerhof, Phys. Rev. Lett **77**, 3865 (1996).

- ²¹ J. P. Perdew, *et al.*, Phys. Rev. B **46**, 6671 (1992).
- ²² P. E. Blöchl, Phys. Rev. B **50**, 17953 (1994).
- ²³ G. Kresse and J. Furthmüller, Phys. Rev. B **54**, 11169 (1996).
- ²⁴ G. Kresse and D. Joubert, Phys. Rev. B **59**, 1758 (1999).
- ²⁵ H. J. Monkhorst and J. Pack, Phys. Rev. B **13**, 5188 (1976).
- ²⁶ P. E. Blöchl, O. Jepsen, and O. K. Andersen, Phys. Rev. B **49**, 16223 (1994).
- ²⁷ I. I. Mazin, *et al.*, (2008), arXiv/0803.2740.
- ²⁸ S. Ishibashi, K. Terakura, and H. Hosono (2008), arXiv/0804.2963.
- ²⁹ F. Ma, Z.-Y. Lu, and T. Xiang (2008), arXiv/0804.3370.
- ³⁰ T. Yildirim (2008), arXiv/0804.2252.
- ³¹ I. I. Mazin, *et al.*, Phys. Rev. B **78**, 085104 (2008).
- ³² H.-J. Grafe, *et al.*, arXiv/0805.2595 (2008).
- ³³ B. Lorenz, *et al.*, (2008), arXiv/0804.1582.
- ³⁴ M. Fratini, *et al.* (2008), arXiv/0805.3992.
- ³⁵ M. A. McGuire, *et al.* (2008), arXiv/0806.3878.
- ³⁶ T. Yildirim (2008), arXiv/0805.2888.
- ³⁷ Y. Ishida, *et al.* (2008), arXiv/0805.2647.
- ³⁸ W. Malaeb, *et al.* (2008), arXiv/0806.3860.
- ³⁹ D. H. Lu, *et al.* (2008), arXiv/0807.2009.
- ⁴⁰ Y. Kamihara, *et al.*, Phys. Rev. B **77**, 214515 (2008).
- ⁴¹ T. M. McQueen, *et al.*, (2008), arXiv/0805.2149.
- ⁴² R. Che, *et al.*, Phys. Rev. B **77**, 184518 (2008).
- ⁴³ M. Tegel, *et al.*, (2008), arXiv/0805.1208.
- ⁴⁴ Z.-A. Ren, *et al.*, arXiv/0804.2582 (2008).
- ⁴⁵ C. Wang, *et al.*, arXiv/0804.4290 (2008).
- ⁴⁶ J.-W. G. B. Bos, *et al.*, arXiv/0806.0926 (2008).
- ⁴⁷ L. Li, *et al.*, arXiv/0806.1675 (2008).